© 2016. Published by The Company of Biologists Ltd | Development (2016) 143, 2398-2409 doi:10.1242/dev.130658

RESEARCH ARTICLE

YAP stabilizes SMAD1 and promotes BMP2-induced neocortical astrocytic differentiation

Zhihui Huang[1,2], Jinxia Hu[1,3,4], Jinxiu Pan[1,3], Ying Wang[1,5], Guoqing Hu[6], Jiliang Zhou[6], Lin Mei[1,3] and Wen-Cheng Xiong[1,3,*]

ABSTRACT

YAP (yes-associated protein), a key transcriptional co-factor that is negatively regulated by the Hippo pathway, is crucial for the development and size control of multiple organs, including the liver. However, its role in the brain remains unclear. Here, we provide evidence for YAP regulation of mouse neocortical astrocytic differentiation and proliferation. YAP was undetectable in neurons, but selectively expressed in neural stem cells (NSCs) and astrocytes. YAP in NSCs was required for neocortical astrocytic differentiation, with no apparent role in self-renewal or neural differentiation. However, YAP in astrocytes was necessary for astrocytic proliferation. *Yap* (*Yap1*) knockout, *Yap*^{nestin} conditional knockout and *Yap*^{GFAP} conditional knockout mice displayed fewer neocortical astrocytes and impaired astrocytic proliferation and, consequently, death of neocortical neurons. Mechanistically, YAP was activated by BMP2, and the active/nuclear YAP was crucial for BMP2 induction and stabilization of SMAD1 and astrocytic differentiation. Expression of SMAD1 in YAP-deficient NSCs partially rescued the astrocytic differentiation deficit in response to BMP2. Taken together, these results identify a novel function of YAP in neocortical astrocytic differentiation and proliferation, and reveal a BMP2-YAP-SMAD1 pathway underlying astrocytic differentiation in the developing mouse neocortex.

KEY WORDS: YAP, BMP2, SMAD1, Astrocytes, Differentiation, Proliferation

INTRODUCTION

The conserved Hippo pathway regulates organ size and tumorigenesis by negatively regulating the oncogenic transcriptional co-activators yes-associated protein (YAP, or YAP1) and TAZ (WWTR1) (Pan, 2010; Mo et al., 2014; Piccolo et al., 2014). Upon stimulation, the Hippo pathway subsequently phosphorylates YAP, and phosphorylated YAP undergoes degradation or interacts with 14-3-3 for its cytoplasmic retention. When dephosphorylated, YAP enters the nucleus and interacts with TEAD family proteins to induce the transcription of genes that regulate diverse cellular processes, including cell survival, proliferation and differentiation (Zhao et al., 2007; Lian et al., 2010; Pan, 2010; Schlegelmilch et al., 2011; Tamm et al., 2011; Liu et al., 2012; Yu and Guan, 2013; Mo et al., 2014; Piccolo et al., 2014; Varelas, 2014; Yao et al., 2014; Ohgushi et al., 2015). Although the function of YAP in regulating the development of multiple organs has been investigated, its role in the developing nervous system is less well studied.

Astrocytes emerge as a type of glial cells crucial for a wide variety of functions in the CNS, including promoting neuronal survival (Sofroniew and Vinters, 2010). During brain development, astrocytes and neurons are derived from the same pool, namely the neural stem cells (NSCs) that reside in the ventricular zone (Temple, 2001; Kriegstein and Alvarez-Buylla, 2009). Rodent cortico-cerebral astrogliogenesis mainly takes place during the first postnatal week, following neurogenesis (Mallamaci, 2013), and comprises two concurrent regulatory processes: (1) determination of astrocyte progenitor cell fate (astrocyte differentiation); and (2) the local proliferation of astrocytes (Ge et al., 2012; Mallamaci, 2013). Although recent *in vitro* and mouse model studies indicate that the bone morphogenetic protein (BMP)-Smad (Gross et al., 1996; Bond et al., 2012; Mallamaci, 2013), Notch (Morrison et al., 2000; Mallamaci, 2013) and Janus kinase-signal transducer and activator of transcription (JAK-STAT) signaling pathways control the appropriate timing of astrogliogenesis (Bonni et al., 1997; He et al., 2005), exactly how these pathways regulate astrogliogenesis remains poorly understood.

Here, we provide evidence for YAP function in the regulation of mouse neocortical astrocytic differentiation and proliferation during brain development. YAP was selectively expressed in NSCs and astrocytes. *Yap* (*Yap1*) conditional knockout (CKO) mouse models, *Yap*^{nestin}-CKO and *Yap*^{GFAP}-CKO, displayed fewer neocortical astrocytes and impaired astrocytic proliferation, whereas YAP-deficient NSCs showed normal self-renewal activity and neural differentiation. Further mechanistic studies showed that YAP was required for BMP2-induced stabilization of SMAD1 and astrocytic differentiation. Taken together, these results identify a novel function of YAP that is crucial in promoting neocortical astrocytic differentiation and proliferation during mouse brain development.

RESULTS

Selective expression of YAP in NSCs and astrocytes in the developing mouse neocortex

To understand how YAP regulates brain development, we first examined its expression pattern in mouse brain by immunohistochemical staining. In P1 wild-type (WT) neocortex, YAP-positive signal was detected largely in BLBP^{+} cells (Fig. 1A, arrows indicate typical examples; BLBP is also known as FABP7) and aldolase C^{+} cells (Fig. 1B), both markers for postnatal

[1]Department of Neuroscience & Regenerative Medicine and Department of Neurology, Medical College of Georgia, Augusta, GA 30912, USA. [2]Institute of Hypoxia Medicine and Institute of Neuroscience, Wenzhou Medical University, Wenzhou, Zhejiang 325035, China. [3]Charlie Norwood VA Medical Center, Augusta, GA 30912, USA. [4]Institute of Nervous System Diseases, Xuzhou Medical College, Xuzhou, Jiangsu 221002, China. [5]Research Center of Blood Transfusion Medicine, Key Laboratory of Laboratory Medicine (Wenzhou Medical University), Ministry of Education, Zhejiang Provincial People's Hospital, Hangzhou, Zhejiang 310014, China. [6]Department of Pharmacology and Toxicology, Medical College of Georgia, Augusta, GA 30912, USA.

*Author for correspondence (wxiong@gru.edu)

W.-C.X., 0000-0001-9071-7598

Received 8 September 2015; Accepted 16 May 2016

Development (2016) 143, 2398-2409 doi:10.1242/dev.130658

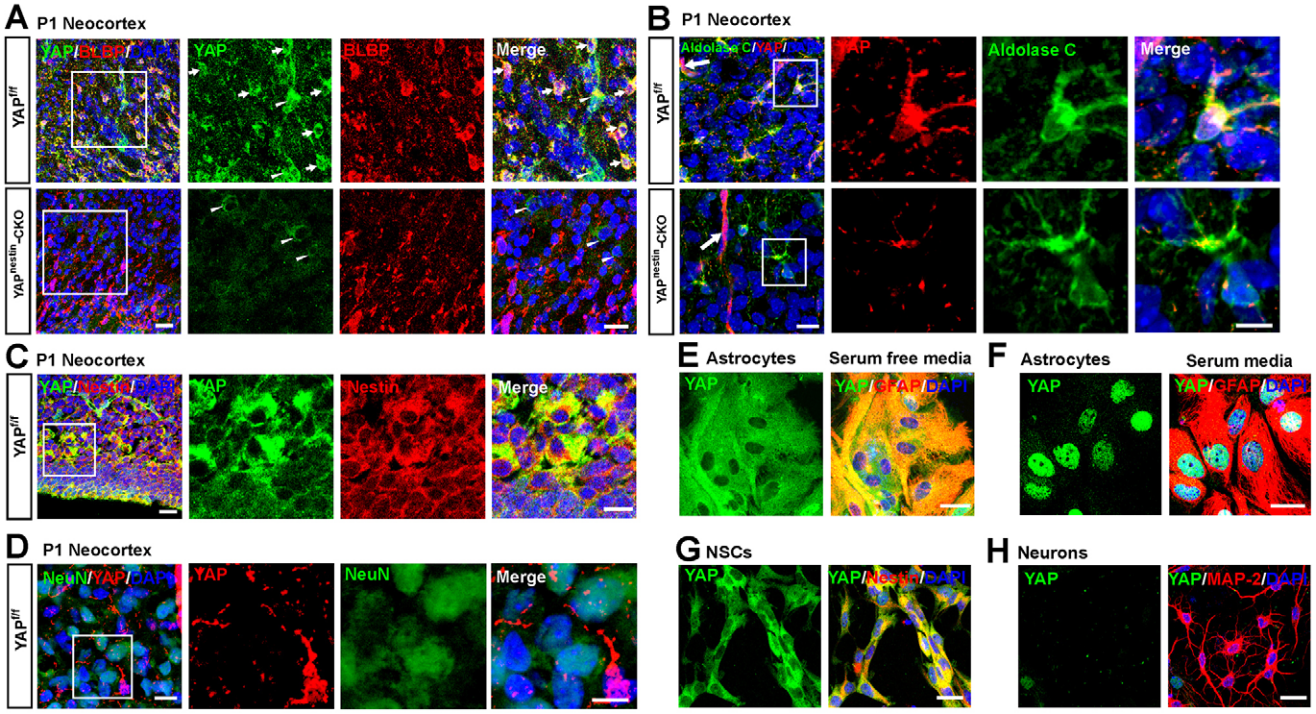

Fig. 1. Selective expression of YAP in neocortical NSCs and astrocytes. (A) Double immunostaining of YAP (green) and BLBP (red) in the layer III-V neocortex of P1 *Yap*$^{f/f}$ and *Yap*^{nestin}-CKO mice. Arrows and arrowheads indicate typical YAP^{+}/BLBP^{+} and YAP^{+}/BLBP^{-} cells, respectively. The boxed region is magnified to the right as single-channel and merged images. (B) Double immunostaining of YAP (red) and aldolase C (green) in the neocortex of P1 *Yap*$^{f/f}$ and *Yap*^{nestin}-CKO mice. Arrows indicate the blood vessels. (C,D) Double immunostaining of (C) YAP (green) and nestin (red) and (D) YAP (red) and NeuN (green) in the neocortex of P1 *Yap*$^{f/f}$ mice. (E,F) Double immunostaining of YAP (green) and GFAP (red) in primary cultured astrocytes with (E) serum-free medium or (F) 10% FBS+DMEM. (G,H) Double immunostaining of (G) YAP (green) and nestin (red) in primary cultured NSCs or (H) YAP (green) and MAP2 (red) in primary cultured neocortical neurons (4 days *in vitro*) from WT neocortex. DAPI (blue) was used to stain nuclei. The YAP antibody used in B and D was from CST (#8418/D24E4), otherwise from Sigma (WH0010413M1). Scale bars: 20 µm.

neocortical astrocytes, as well as in nestin^{+} (an NSC marker) cells (Fig. 1C). Note that YAP was detected in a few BLBP^{-} cells (Fig. 1A, arrowheads indicate typical examples). However, YAP was undetectable in NeuN^{+} (a marker for neurons, also known as RBFOX3) cells (Fig. 1D). These BLBP^{-}/YAP^{+} cells might be endothelial cells of blood vessels. These results thus indicate YAP expression in astrocytes and NSCs, but not in neurons, in line with a previous report (Serinagaoglu et al., 2015). It is also important to note that the YAP/TAZ immunopositive signals in astrocytes and NSCs, but not blood vessels, were markedly reduced in *Yap*^{nestin}-CKO neocortex (Fig. 1A,B; data not shown), demonstrating the specificity of YAP antibodies.

To further verify YAP expression in NSCs and astrocytes, but not neurons, we used primary cultured brain cells, including nestin^{+} NSCs and their derivatives, such as neurons and astrocytes. Indeed, double immunostaining analysis of YAP and cell type-specific markers showed that YAP was detected in most of the GFAP^{+} astrocytes (Fig. 1E,F) and nestin^{+} NSCs (Fig. 1G), but not in MAP2^{+} neurons (Fig. 1H). Interestingly, YAP protein was mainly distributed in the cytoplasm of NSCs (Fig. 1G) but in the nuclei of astrocytes under the culture condition with serum (10% FBS+DMEM) (Fig. 1F). When cultured in serum-free DMEM, the astrocytic YAP was mainly distributed in the cytoplasm (Fig. 1E). YAP expression in NSCs and astrocytes, but not neurons, was further verified by western blot analysis (data not shown).

Finally, western blot analysis showed that YAP expression in the neocortex reached a peak level in postnatal weeks 2-3, which matched well with astrocyte development (Fig. S1A,B). Together, these results demonstrate selective YAP expression in NSCs and astrocytes in culture and in mouse brain.

Normal NSC proliferation in YAP-deficient NSCs

YAP is believed to be crucial for the self-renewal of embryonic stem cells (Lian et al., 2010; Pan, 2010; Schlegelmilch et al., 2011; Tamm et al., 2011; Liu et al., 2012; Mo et al., 2014; Piccolo et al., 2014; Pijuan-Galito et al., 2014; Varelas, 2014; Yao et al., 2014; Ohgushi et al., 2015). These observations and the high level of YAP in nestin^{+} NSCs led to the hypothesis that YAP might promote NSC self-renewal or proliferation. To test this hypothesis, we used neurosphere cultures derived from *Yap*$^{f/f}$ and *Yap*^{nestin}-CKO neocortex (at E14.5). Again, YAP was expressed in NSCs from *Yap*$^{f/f}$, but not *Yap*^{nestin}-CKO, embryos, and was largely distributed in the cytoplasm of NSCs, with a few nuclear YAP^{+} cells at the edge of neurospheres (Fig. 2A,B). In viewing the size of neurospheres of the two genotypes, no obvious difference was apparent even in the fifth passages of the NSC culture (Fig. 2A,C), implicating normal growth of NSCs.

We next examined cell proliferation in dissociated NSCs from neurospheres, which were plated onto poly-L-ornithine- and fibronectin-coated coverslips in media containing bFGF (FGF2) and EGF to keep the NSCs in a monolayer. Comparable numbers of Ki67^{+} and phospho-histone H3 (PH3)$^{+}$ (markers of proliferative cells) cells were observed in *Yap*$^{f/f}$ and *Yap*^{nestin}-CKO NSC cultures (Fig. 2D-G), suggesting little, if any, role of YAP in regulating NSC proliferation in culture. This view was further supported by *in vivo* immunohistochemical staining and stereological analyses of PH3^{+} cells in E14.5 *Yap*$^{f/f}$ and *Yap*^{nestin}-CKO neocortex (Fig. 2H,I).

Development (2016) 143, 2398-2409 doi:10.1242/dev.130658

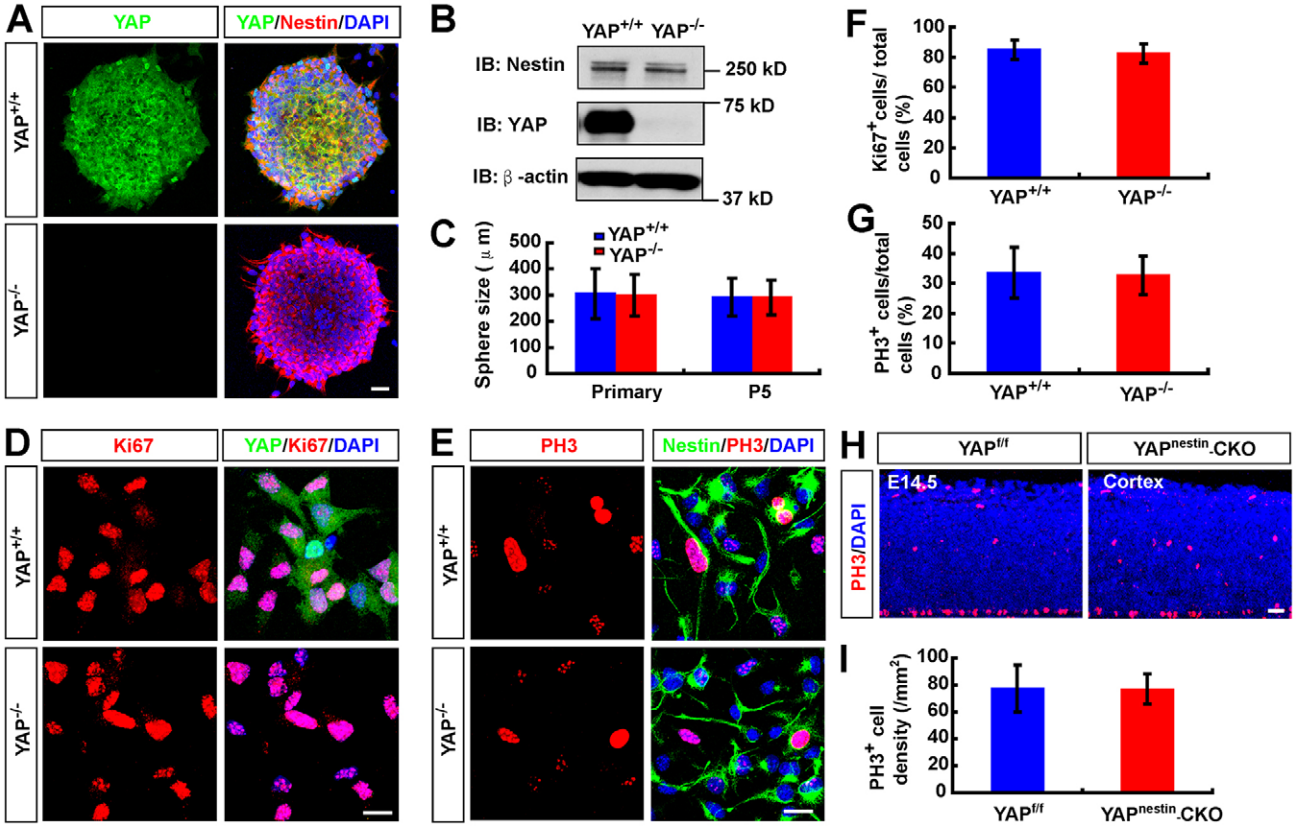

Fig. 2. Normal proliferation and self-renewal of NSCs in *Yap*^{nestin}-CKO mice. (A) Double immunostaining of YAP (green) and nestin (red) in cultured neurospheres from E14.5 *Yap*$^{f/f}$ and *Yap*^{nestin}-CKO mice. (B) Western blot analysis of YAP expression in WT and YAP-deficient neurospheres. IB, immunoblot antibody. (C) Quantification of WT and YAP-deficient neurosphere size in primary cultures or the fifth passage of the primary cultures (n=100 per group). (D,E) Double immunostaining analysis of (D) Ki67 (red) and YAP (green) or (E) PH3 (red) and nestin (green) in NSCs from WT and YAP-deficient neurospheres. (F,G) Quantitative analysis of the percentage of (F) Ki67$^+$ cells (n=45 fields per group) and (G) PH3$^+$ cells (n=30 fields per group) among total WT or YAP-deficient NSCs. (H) Immunostaining analysis of PH3 in the neocortex of E14.5 *Yap*$^{f/f}$ and *Yap*^{nestin}-CKO mice. (I) Quantitative analysis of PH3$^+$ cells in *Yap*$^{f/f}$ and *Yap*^{nestin}-CKO mice (n=8 sections in WT group, n=6 sections in mutant group). DAPI (blue) was used to stain nuclei. Data are mean±s.d. Scale bars: 20 μm.

Consistently, deletion of *Yap* did not affect their mitotic division (Fig. S2A-D). Taken together, these observations suggest that YAP may not be required in nestin$^+$ NSCs for their proliferation or self-renewal in culture and *in vivo*.

Impaired astrocytic differentiation in YAP-deficient NSCs

We next asked whether YAP plays a role in neurogenesis. Neurospheres were plated on coverslips coated with poly-L-ornithine and cultured in neurobasal medium plus 2% B27 without bFGF and EGF to induce neuronal differentiation. Tuj1$^+$ (a marker for neurons, also known as TUBB3) cells were induced in both YAP$^+$ and YAP-deficient cultures (Fig. 3A). No significant difference was detected between YAP$^+$ and *Yap* mutant cultures based on the quantification of Tuj1$^+$ neuron numbers and Tuj1 protein level (Fig. 3A-C), suggesting that YAP in nestin$^+$ NSCs might not be required for neurogenesis in culture.

We then determined whether YAP regulates astrocytic differentiation. Neurospheres plated on coverslips coated with poly-L-ornithine were incubated with 10% FBS to induce astrocyte differentiation (Obayashi et al., 2009). As shown in Fig. 3D,E, GFAP$^+$ astrocytes were induced from the NSCs of *Yap*$^{f/f}$ embryos, but they were obviously reduced in *Yap*^{nestin}-CKO cultures. The decrease in GFAP protein level was also detected in homogenates of astrocytes derived from *Yap*^{nestin}-CKO NSCs, as compared with that of *Yap*$^{f/f}$ controls (Fig. 3F,G). These results indicate impaired astrocytic differentiation in YAP-deficient NSC cultures. Together, these results suggest that YAP expression in nestin$^+$ NSCs is necessary for astrocytic differentiation but not for NSC proliferation or neurogenesis.

Reduced proliferation of neocortical astrocytes in *Yap*^{nestin}-CKO brain

In addition to NSCs, YAP is expressed in astrocytes (Fig. 1A,B,E,F). To examine YAP function in astrocytes, we first examined whether it is required for astrocytic proliferation. When primary astrocytes from P1 *Yap*$^{f/f}$ and *Yap*^{nestin}-CKO mice were cultured, the YAP-deficient astrocytes appeared to proliferate at a slower rate than *Yap*$^{f/f}$ astrocytes. To avoid cell density effects on astrocytic proliferation, we replated YAP$^+$ and YAP-deficient astrocytes at the same density on coverslips and after overnight culture stained for GFAP, Ki67 and PH3. Indeed, marked reductions in Ki67$^+$ and PH3$^+$ astrocytes were detected in *Yap* mutant culture, as compared with controls (Fig. 4A-D), indicating that YAP is necessary for astrocytic proliferation in culture.

To determine whether YAP is involved in astrocytic proliferation *in vivo*, we carried out BrdU injection experiments to mark proliferative cells. First, BrdU was injected into pregnant mothers at ~E14.5, and P1 pups were examined (Fig. 4E). Co-immunostaining analysis of Ki67 and BrdU revealed a marked reduction of Ki67$^+$ cells in the neocortex of *Yap*^{nestin}-CKO mice compared with *Yap*$^{f/f}$ controls (Fig. 4F,G). However, BrdU$^+$ cells were present at comparable levels in the neocortex of WT and *Yap*

Development (2016) 143, 2398-2409 doi:10.1242/dev.130658

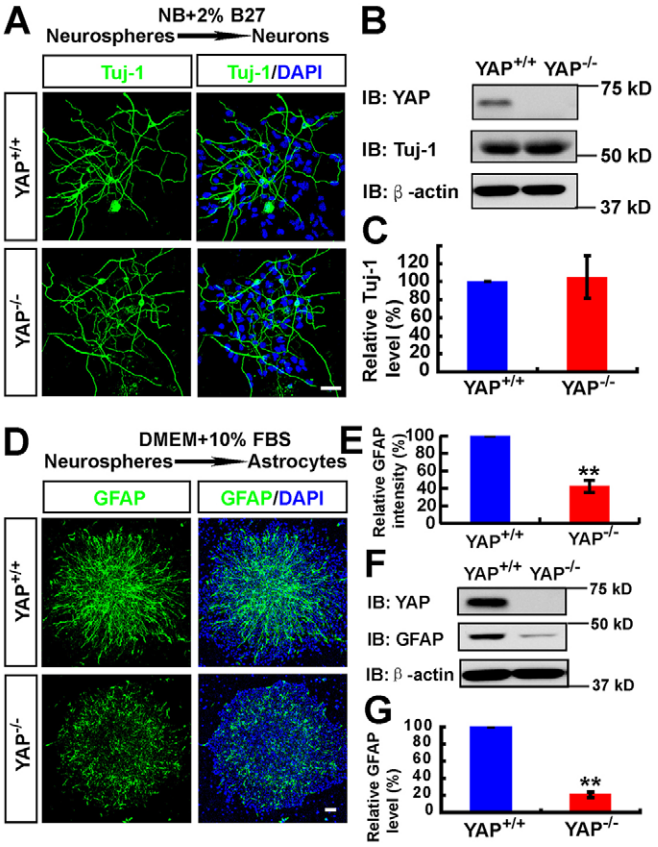

Fig. 3. Impaired astrocytic differentiation, but normal neuronal differentiation, in YAP-deficient NSCs. (A) Immunostaining analysis of Tuj1 (green) in neurons differentiated from WT and YAP-deficient neurospheres (by incubating with neurobasal medium plus 2% B27). (B) Western blot analysis of Tuj1 in neurons differentiated from WT and YAP-deficient neurospheres. (C) Quantitative analysis of western blot data (n=3 per group, normalized to the WT group) as shown in B. (D) Immunostaining analysis of GFAP (green) in astrocytes differentiated from WT and YAP-deficient neurospheres (by incubating with DMEM plus 10% FBS). (E) Quantitative analysis of the relative GFAP intensity (normalized to the WT group, n=6) as shown in D. (F) Western blot analysis of GFAP expression in astrocytes differentiated from WT and YAP-deficient neurospheres. (G) Quantitative analysis of western blot data (n=4 per group, normalized to the WT group) as shown in F. Data are mean±s.e.m. $^{**}P<0.01$, compared with control group, Student's t-test. Scale bars: 20 µm.

mutant mice (Fig. 4F,H), suggesting that YAP might be required for postnatal cell proliferation but not for the proliferation of embryonic NSCs.

Since local proliferation constitutes a major astrocyte source in the postnatal neocortex (Ge et al., 2012), we next examined whether local proliferation of astrocytes is impaired by *Yap* deletion. BrdU was injected into P1 and P7 mice and 2 h after injection the brains were examined (Fig. 4I, Fig. S3A). Co-immunostaining analysis of BrdU with BLBP (a marker not only for radial glia during embryonic development, but also for astrocytes in the postnatal neocortex) (Guo et al., 2009; Ge et al., 2012) showed a significant reduction of $BrdU^+$ cells and BLBP/BrdU double-positive cells in the neocortex of Yap^{nestin}-CKO mice compared with WT controls (Fig. 4J-L, Fig. S3B-D). Note that our results also showed fewer $Ki67^+$ (P0 staining; Fig. 4F,G) and $BrdU^+$ (P1 injection; Fig. 4J,K) cells in the intermediate zone-subventricular zone layers of the neocortex. These proliferative cells include NSCs and astrocyte precursors. Thus, it is possible that YAP regulates both astrocyte and postnatal NSC proliferation. Taken together, these results suggest that YAP is also required for the local proliferation of neocortical astrocytes.

Impaired neocortical astrogliogenesis in Yap^{nestin}-CKO and Yap^{GFAP}-CKO mice

To further determine YAP function in astrogliogenesis *in vivo*, we compared astrocyte number and morphology in $Yap^{f/f}$ and Yap^{nestin}-CKO brain sections. As shown in Fig. 5A,B, $BLBP^+$ cells were markedly reduced in the neocortex of Yap^{nestin}-CKO mice. However, $BLBP^+$ cells were not decreased in the hippocampus of Yap^{nestin}-CKO mice (Fig. 5A,B). Moreover, BLBP protein was selectively reduced in the mutant neocortex, but not hippocampus (Fig. 5C,D). Aldolase C^+ cells (another astrocyte marker) (Molofsky et al., 2012) were also markedly reduced in the neocortex, but not hippocampus, of Yap^{nestin}-CKO mice (Fig. 5E-G). These results suggest that YAP might be selectively involved in neocortical astrogliogenesis.

To further confirm YAP functions in neocortical astrogliogenesis, we generated another *Yap* knockout allele, Yap^{GFAP}-CKO, by crossing $Yap^{f/f}$ with GFAP-Cre. GFAP-Cre drives Cre expression under the control of the *Gfap* promoter, which is more selectively expressed in astrocytes than elsewhere (Gavériaux-Ruff and Kieffer, 2007). As in Yap^{nestin}-CKO mice, YAP expression was largely decreased in brain regions in Yap^{GFAP}-CKO mice, including the olfactory bulb, midbrain, neocortex, hippocampus and cerebellum (Fig. S4A,B), and abolished in cultured Yap^{GFAP}-CKO astrocytes (Fig. S4C,D). The primary astrocytes from Yap^{GFAP}-CKO mice displayed reduced cell proliferation, compared with WT controls (Fig. S5A-D). In agreement with the phenotypes detected in Yap^{nestin}-CKO mice, Yap^{GFAP}-CKO mice showed decreased neocortical astrocytic proliferation (Fig. S5E,G) and fewer neocortical astrocytes (Fig. S5F,H). These observations thus provide additional support for the proposal that YAP is necessary to promote neocortical astrogliogenesis. Taken together, these results suggest that YAP may selectively regulate neocortical astrogliogenesis, but not hippocampal astrogliogenesis or neuronal differentiation.

Increased neocortical neurodegeneration in the Yap^{nestin}-CKO brain

In addition to astrocytes, we examined neocortical and neuronal morphology by Nissl staining analysis. At P0-P1, neocortical morphology and the neural layers appeared to be normal (Fig. 6A,B). However, at P7, the neocortex became thinner in Yap^{nestin}-CKO brain compared with control ($Yap^{f/f}$) mice, and the neuronal density, particularly in neocortical layers IV-VI, was significantly reduced (Fig. 6A,B). Additionally, $CUX1^+$ (a marker of neocortical layers II-IV) and $NeuN^+$ cells in layers IV-VI were significantly decreased in P7 Yap^{nestin}-CKO mice compared with controls ($Yap^{f/f}$) (Fig. 6C-E). Again, this phenotype was not observed in P0-P1 mutant brain, as $NeuN^+$, $TBR1^+$ and $TBR2^+$ (neocortical layer marker, also known as EOMES) cells appeared to be unchanged in Yap^{nestin}-CKO compared with $Yap^{f/f}$ mice (Fig. S6A,B). These results suggest that *Yap* deletion might cause neocortical neuronal loss.

This view was further supported by the observations that Fluoro-Jade C (a maker of degenerating neurons) signal was detected in P7 Yap^{nestin}-CKO mice, but not in the controls (Fig. 6F,G), and that active caspase 3 (a marker of apoptosis) staining was also elevated in mutant neocortex (Fig. 6H,I). Moreover, the neocortex became thinner in Yap^{GFAP}-CKO brain compared with control ($Yap^{f/f}$) mice,

Development (2016) 143, 2398-2409 doi:10.1242/dev.130658

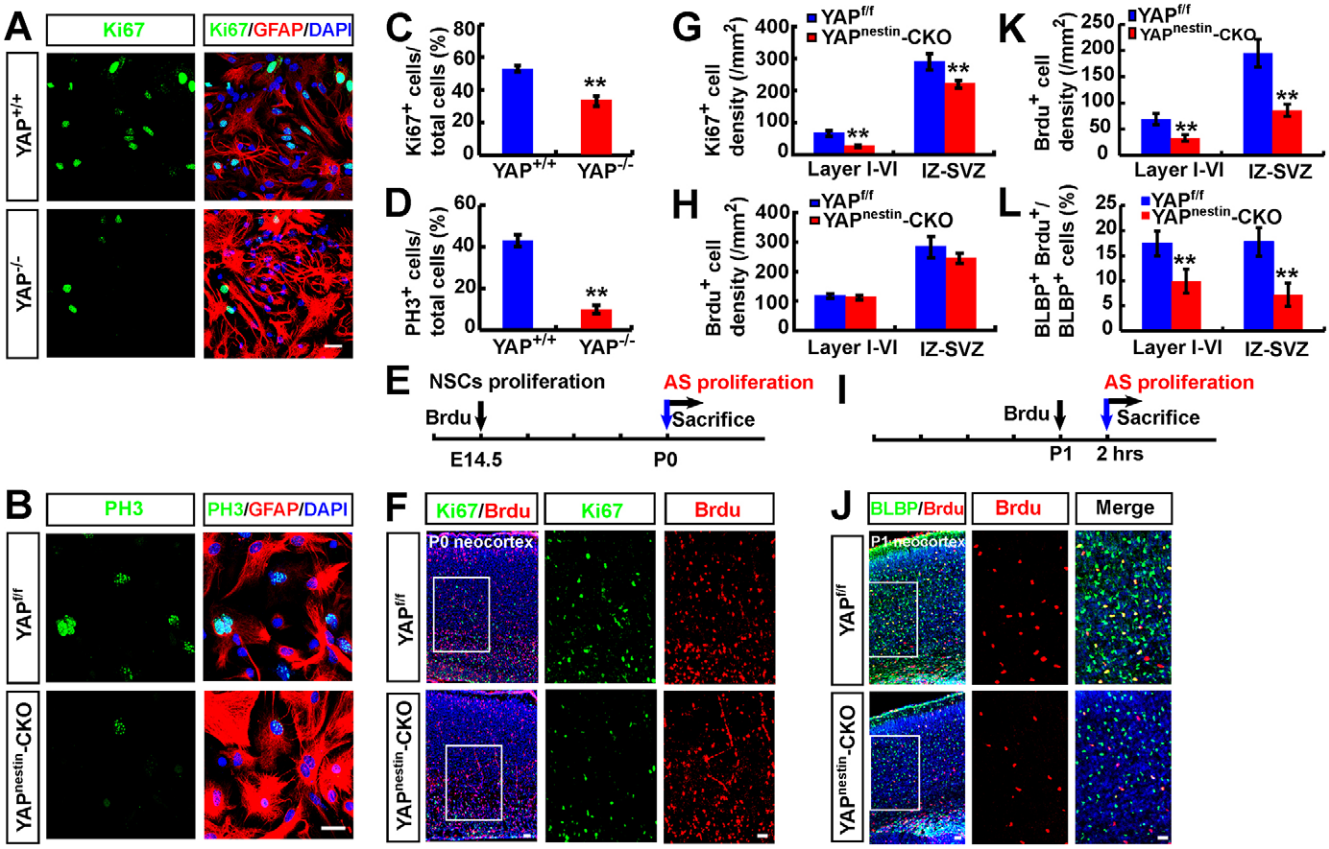

Fig. 4. Reduced local proliferation of neocortical astrocytes in *Yap*^{nestin}-CKO mice. (A,B) Double immunostaining analysis of (A) Ki67 (green) and GFAP (red) or (B) PH3 (green) and GFAP (red) in cultured astrocytes from P1 *Yap*$^{f/f}$ and *Yap*^{nestin}-CKO mice. (C,D) Quantitative analysis of the percentage of Ki67^{+} (C, *n*=16 per group) and PH3^{+} (D, *n*=12 per group) astrocytes among total astrocytes. (E) Scheme of BrdU incorporation experiments in F. AS, astrocyte. (F) Double immunostaining analysis of Ki67 (green) and BrdU (red) in neocortex of P0 *Yap*$^{f/f}$ and *Yap*^{nestin}-CKO mice (sagittal sections). (G,H) Quantitative analysis of (G) Ki67^{+} or (H) BrdU^{+} cell density in neocortex of P0 *Yap*$^{f/f}$ and *Yap*^{nestin}-CKO mice (*n*=4 per group) as shown in F. (I) Scheme of BrdU incorporation experiments in J. (J) Double immunostaining analysis of BLBP (green) and BrdU (red) in neocortex of P1 *Yap*$^{f/f}$ and *Yap*^{nestin}-CKO mice (sagittal sections). (K,L) Quantitative analysis of (K) BrdU^{+} cell density and (L) the percentage of BLBP^{+} and BrdU^{+} cells among total BLBP^{+} cells (*n*=10 per group) in neocortex of P1 *Yap*$^{f/f}$ and *Yap*^{nestin}-CKO mice as shown in J. Boxed regions are shown at higher magnification. DAPI (blue) was used to stain nuclei. Data are mean±s.e.m. $^{**}P<0.01$, compared with control group, Student's *t*-test. Scale bars: 20 µm.

and the neuronal density, particularly in neocortical layers IV-VI, was significantly reduced (Fig. S7A,B). Taken together, these results demonstrate neocortical neurodegeneration in the mutant brain, which may be a consequence of impaired astrogliogenesis.

Requirement of YAP for BMP2-induced astrocytic differentiation

The BMP2 signaling pathway is crucial for astrocytic differentiation (Gross et al., 1996; Mallamaci, 2013) and YAP is required for BMP2 signaling in HaCaT cells or mouse embryonic stem cells (Alarcón et al., 2009; Aragon et al., 2011; Yao et al., 2014). We thus examined whether YAP is required for BMP2-induced astrocytic differentiation in NSCs. Cultured NSCs plated on coverslips were treated with BMP2 to induce astrocytic differentiation. Interestingly, GFAP^{+} astrocytes were induced from NSCs of control embryos at day 3 after BMP2 treatment, whereas they were reduced in YAP-deficient cultures (Fig. 7A,B). These results support the view that YAP in NSCs is required for BMP2-induced astrocytic differentiation.

We next examined whether BMP2 downstream signaling (e.g. pSMAD1/5/8) in NSCs is impaired by *Yap* deletion. As shown in Fig. 7C-F, pSMAD1/5/8 was induced by BMP2 in control NSCs in a time-dependent manner, and YAP protein was also increased by BMP2 stimulation, whereas the ratio of pYAP/YAP was decreased by BMP2 stimulation. By contrast, the BMP2-induced pSMAD1/5/8 and SMAD1 levels were reduced in YAP-deficient NSCs, compared with control NSCs (Fig. 7C,F,G). The decrease in pSMAD1/5/8 is likely to be due to the reduction of SMAD1 protein. The reductions in BMP2-induced pSMAD1/5/8 and SMAD1 were also detected in YAP-deficient astrocytes (Fig. S8A-D). Furthermore, the reduced pSMAD1/5/8 immunosignal was apparent in aldolase C^{+} astrocytes in P1 *Yap* mutant neocortex (Fig. S8E,F). These results suggest that YAP in both NSCs and astrocytes is required to maintain BMP2-induced SMAD1 protein levels, and that YAP in NSCs is also necessary for BMP2-induced astrocytic differentiation.

YAP is necessary for BMP2 induction and stabilization of SMAD1 signaling

How does YAP regulate BMP2-Smad signaling? We first examined whether BMP2 'activates' YAP by promoting YAP nuclear translocation. Indeed, double immunostaining analysis showed increased nuclear translocation of YAP in both WT NSCs and WT astrocytes stimulated by BMP2 (Fig. 7H, Fig. 8A,B), where YAP colocalized with pSMAD1/5/8 (Fig. 7H, Fig. 8A). Again, the pSMAD1/5/8 level was significantly decreased in YAP-deficient cells in response to BMP2 (Fig. 7H, Fig. 8A,B). We further tested

Development (2016) 143, 2398-2409 doi:10.1242/dev.130658

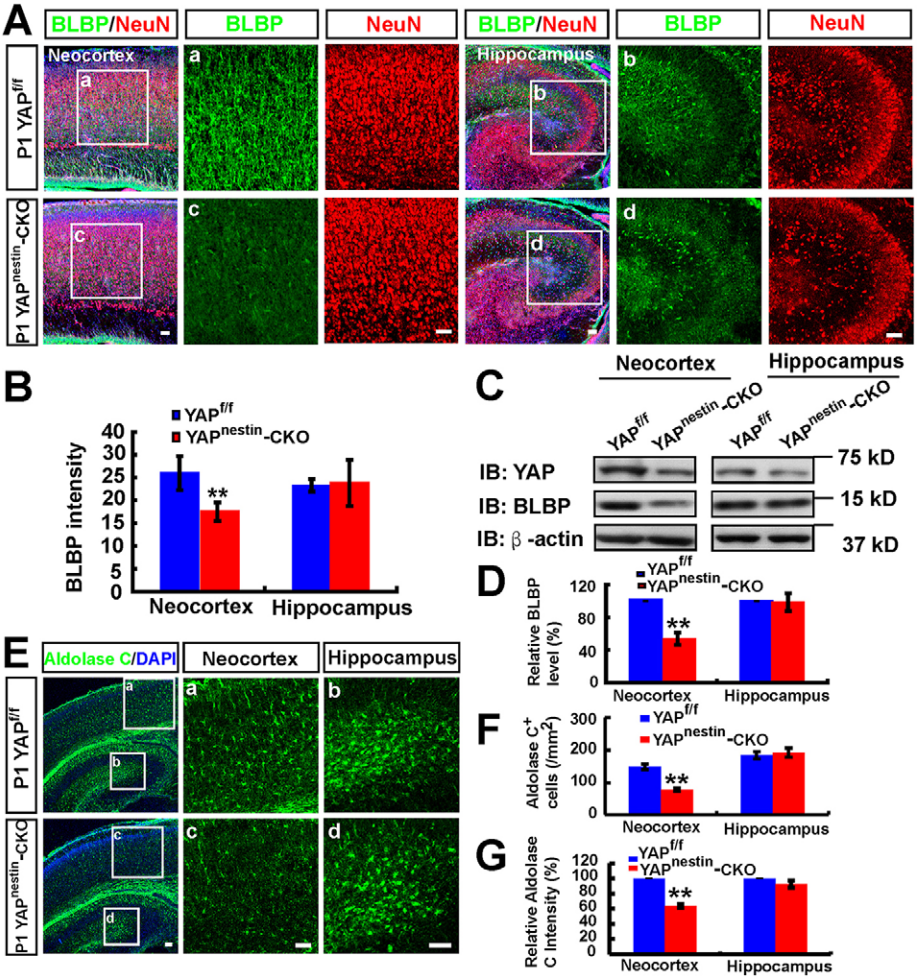

Fig. 5. Reduced neocortical astrogliogenesis in *Yap*^{nestin}-CKO mice. (A) Double immunostaining of BLBP (green) and NeuN (red) in neocortex and hippocampus of P1 *Yap*$^{f/f}$ and *Yap*^{nestin}-CKO mice (sagittal sections). (B) Quantitative analysis of BLBP (*n*=18 for neocortex per group, and *n*=5 for hippocampus per group) fluorescence intensity as shown in A. (C) Western blot analysis of BLBP expression in neocortex and hippocampus of P1 *Yap*$^{f/f}$ and *Yap*^{nestin}-CKO mice. (D) Quantitative analysis of western blot data as shown in C (*n*=3 per group, normalized to WT). (E) Immunostaining of aldolase C (green) in neocortex and hippocampus of P1 *Yap*$^{f/f}$ and *Yap*^{nestin}-CKO mice. (F,G) Quantitative analysis of (F) the density of aldolase C^{+} cells and (G) the relative aldolase C fluorescence intensity (*n*=8 per group, normalized to WT) as shown in E. Selected regions in *Yap*$^{f/f}$ (a,b) and *Yap*^{nestin}-CKO (c,d) mice are shown at higher magnification. Data are mean±s.e.m. $^{**}P<0.01$, compared with control group, Student's *t*-test. Scale bars: 20 µm.

whether the nuclear YAP forms a complex with SMAD1 by nuclear complex co-immunoprecipitation experiments. YAP was detected in the SMAD1 immuno-complex, which was stimulated by BMP2 in astrocytes (Fig. 8C). Because BMP2 promoted pSMAD1/5/8 and YAP nuclear translocation, there was more SMAD1 and YAP at 30 min compared with time zero. These results suggest YAP 'activation' by BMP2.

Note that total SMAD1 was decreased in YAP-deficient cells before and after BMP2 treatment (Fig. 7C,G, Fig. S7A,D). We thus speculate that YAP as a transcription factor might regulate *Smad1* transcription. However, *Yap* deletion did not affect the basal levels of *Smad1* mRNA or in response to BMP2 (Fig. 8D), excluding regulation at the transcriptional level. We then asked whether YAP regulates SMAD1 protein stability. Astrocytes were incubated with cycloheximide (CHX), an inhibitor of protein synthesis, for various times. Cell lysates were analyzed for SMAD1 expression by western blotting. SMAD1 protein levels were decreased more rapidly in YAP-deficient astrocytes than in controls (Fig. 8E,F), suggesting that SMAD1 is unstable in YAP-deficient cells. We further examined SMAD1 stability in BMP2-stimulated YAP^{+} and YAP-deficient astrocytes. As shown in Fig. 8G,H, SMAD1 protein levels were also degraded more rapidly in YAP-deficient cells than in controls. These results suggest that YAP is required to maintain SMAD1 protein stability in both basal and BMP2-stimulated culture conditions.

We further asked whether YAP regulation of SMAD1 in NSCs is essential for YAP promotion of astrocytic differentiation. Flag-tagged SMAD1 was expressed in YAP^{+} and YAP-deficient NSCs, which were subjected to astrocytic differentiation by BMP2. As shown in Fig. 8I,J, 3 days after BMP2 treatment, more GFAP^{+} astrocytes were detected in YAP^{+} and YAP-deficient NSCs expressing Flag-SMAD1 than in the untransfected YAP^{+} and YAP-deficient NSCs. The impaired astrocytic differentiation in YAP-deficient NSCs was diminished by expressing Flag-SMAD1 (Fig. 8I,J). Taken together, these results suggest that SMAD1 is crucial downstream of YAP in NSCs to promote BMP2-induced astrocyte differentiation.

DISCUSSION

Here, we present evidence for YAP function in neocortical astrocytic differentiation and proliferation and propose a working model, as depicted in Fig. 8K. In this model, YAP is suggested to promote astrocytic proliferation and differentiation by stabilizing BMP2-SMAD1 signaling. This study thus not only identifies a novel function of YAP in neocortical astrocytic proliferation and differentiation during brain development, but also provides new insights into the molecular pathways underlying astrocytic differentiation.

In light of reports that YAP is crucial for the proliferation or self-renewal of embryonic stem cells (Lian et al., 2010; Pan, 2010; Schlegelmilch et al., 2011; Tamm et al., 2011; Liu et al., 2012; Ramos and Camargo, 2012; Mo et al., 2014; Piccolo et al., 2014; Varelas, 2014; Yao et al., 2014), we first tested the hypothesis that *Yap* deletion in NSCs might impair their proliferation or self-renewal. However, to our surprise, several lines of evidence suggest

Development (2016) 143, 2398-2409 doi:10.1242/dev.130658

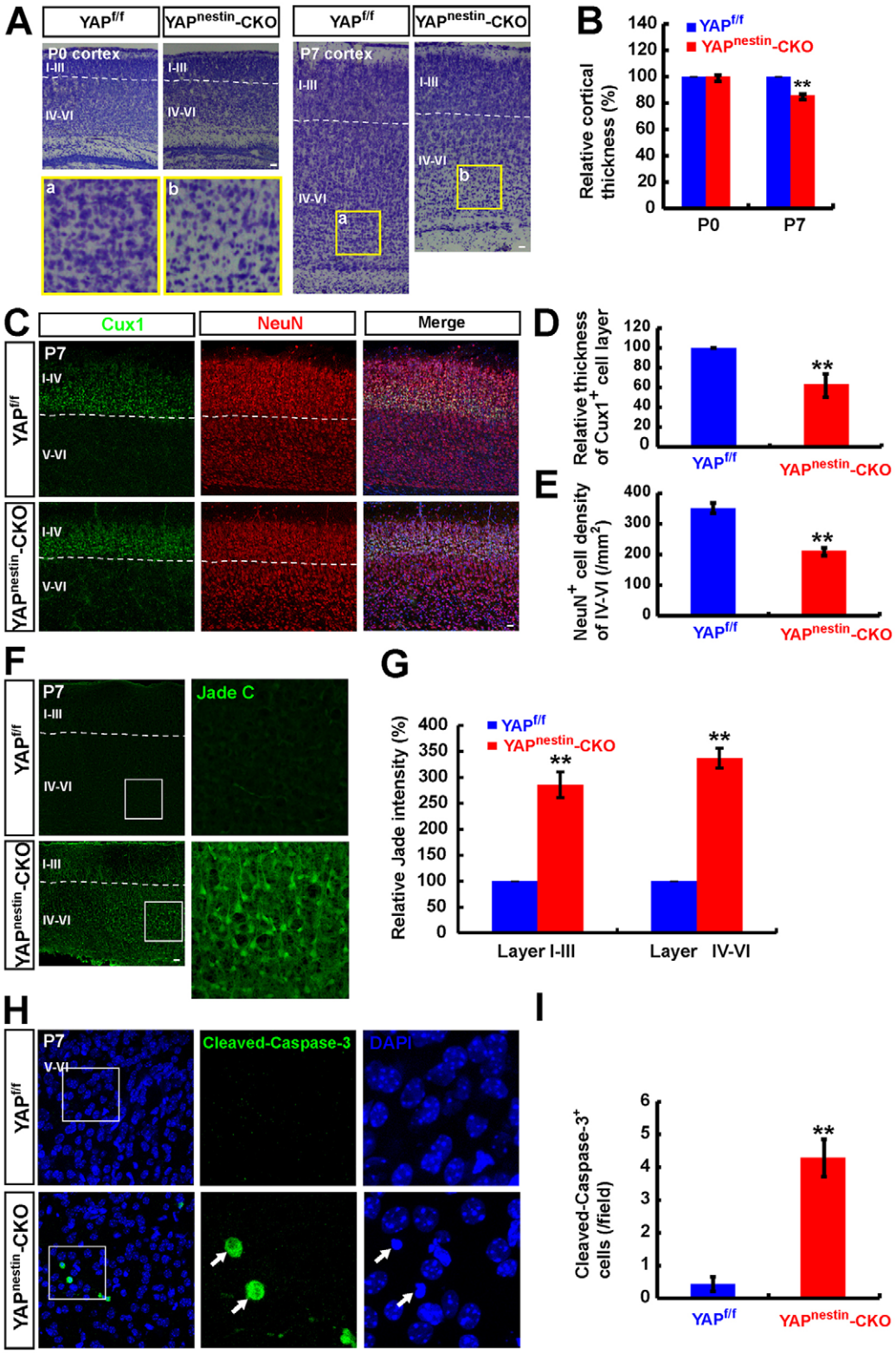

Fig. 6. Increased neocortical neurodegeneration in *Yap*^{nestin}-CKO brain. (A) Nissl stained images (sagittal sections) showing the brain phenotype of P0 and P7 *Yap*$^{f/f}$ and *Yap*^{nestin}-CKO mice. Selected regions in P7 *Yap*$^{f/f}$ (a) and *Yap*^{nestin}-CKO (b) mice are shown at higher magnification. (B) Quantitative analysis of neocortical thickness of P0 and P7 *Yap*$^{f/f}$ and *Yap*^{nestin}-CKO mice (n=25 per group, normalized to WT group). (C) Double immunostaining analysis of CUX1 (green) and NeuN (red) in neocortex of P7 *Yap*$^{f/f}$ and *Yap*^{nestin}-CKO mice (sagittal sections). (D,E) Quantitative analysis of the thickness of the CUX1^{+} cell layer (D, n=9 in *Yap*$^{f/f}$ mice, n=8 in *Yap*^{nestin}-CKO mice) and the density of NeuN^{+} cells of layers IV-VI (E, n=8 per group) as shown in C. (F) Fluoro-Jade C (green) staining in the neocortex of P7 *Yap*$^{f/f}$ and *Yap*^{nestin}-CKO mice. (G) Quantitative analysis of the relative intensity of Fluoro-Jade C (normalized to WT group, n=6 per group) shown in F. (H) Immunostaining analysis of cleaved caspase 3 (green) in layer IV-VI neocortex of P7 *Yap*$^{f/f}$ and *Yap*^{nestin}-CKO mice. (I) Quantitative analysis of the number of cleaved caspase 3^{+} cells in each field (n=7 per group) as shown in H. Boxed regions are shown at higher magnification. Data are mean ±s.e.m. **P<0.01, compared with control group, Student's t-test. Scale bars: 20 µm.

Development (2016) 143, 2398-2409 doi:10.1242/dev.130658

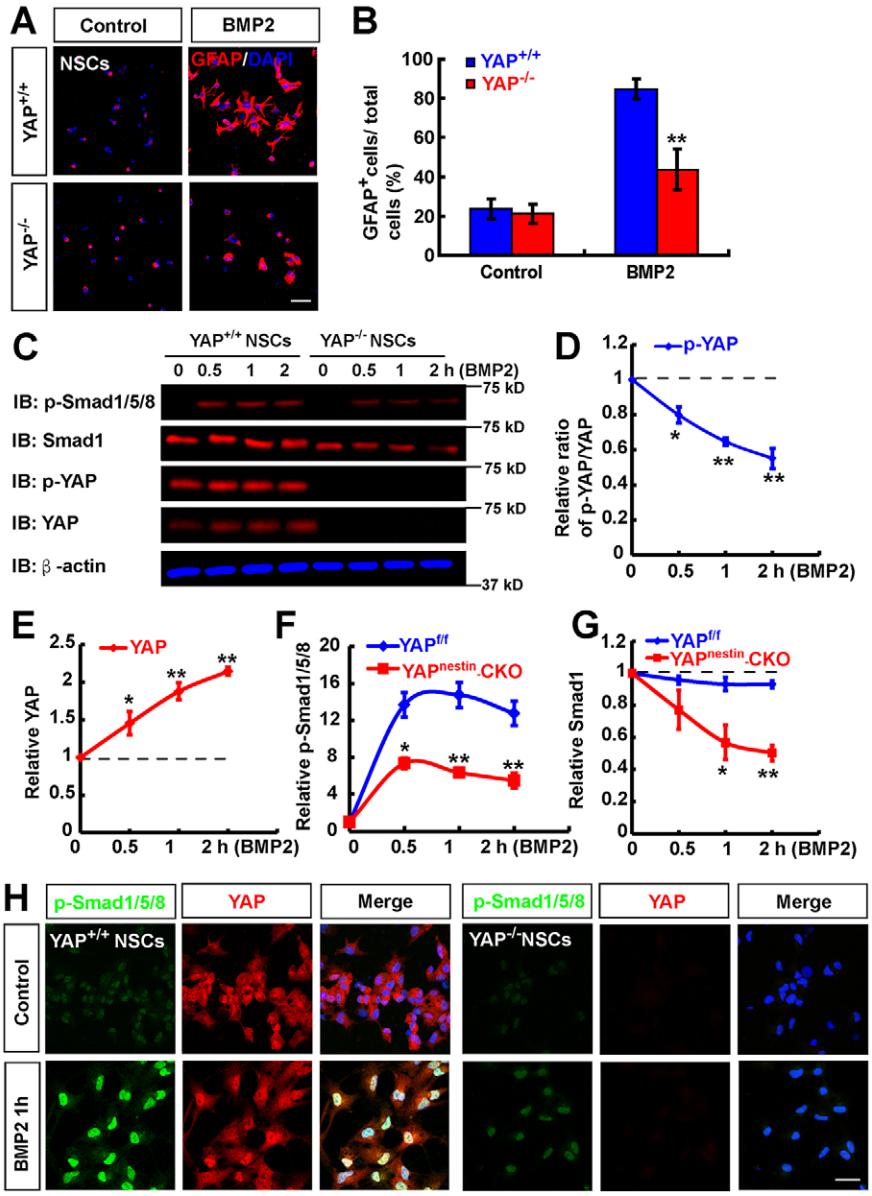

Fig. 7. YAP is required for BMP2-induced astrocytic differentiation. (A) Immunostaining analysis of GFAP (red) in astrocytes differentiated from WT and YAP-deficient NSCs induced by BMP2 treatment (100 ng/ml) for 3 days. (B) Quantitative analysis of the percentage of GFAP$^+$ cells among total cells in one field shown in A (n=12 fields for each group). (C) Western blot to detect signaling downstream of BMP2 in WT and YAP-deficient NSCs before and after BMP2 treatment (100 ng/ml) at the indicated time points. (D-G) Quantitative analysis of the relative ratio of pYAP/YAP (D), relative YAP (E), pSMAD1/5/8 (F) and SMAD1 (G) as shown in C (n=3 per group, normalized to 0 min). (H) Double immunostaining analysis of pSMAD1/5/8 (green) and YAP (red) in WT and YAP-deficient NSCs before and after BMP2 treatment (100 ng/ml). Data are mean±s.e.m. *P<0.05, **P<0.01, compared with control group, Student's t-test. Scale bars: 20 µm.

little to no role for YAP in regulating NSC proliferation. First, in the EGF- and bFGF-dependent neurosphere culture system, neurosphere formation and cell proliferation appeared to be normal in YAP-deficient NSCs, as compared with WT controls (Fig. 2). Second, PH3 staining and BrdU injection into embryonic *Yap*^{nestin}-CKO mice showed comparable levels of proliferative NSCs in the mutant neocortex and controls (Figs 2 and 4). Third, YAP was largely distributed in the cytoplasm of NSCs (Fig. 1C,G, Fig. S2), whereas it is believed that nuclear YAP is essential for cell proliferation (Yu and Guan, 2013; Piccolo et al., 2014). The view that YAP is not necessary for NSC proliferation is also in line with recent observations of unchanged proliferation of stem cells in mammary glands (Chen et al., 2014), pancreas (Zhang et al., 2014) and intestines (Azzolin et al., 2014) upon conditional genetic inactivation of *Yap* (Piccolo et al., 2014). Also noteworthy is that this view appears to differ from reports that EGF activates YAP to promote cell proliferation through activation of Ras-MAPK and PI3K-PDK1 signaling in immortalized mammary cells (Fan et al., 2013; Gumbiner and Kim, 2014). Such differing conclusions might be a result of the different cell types tested. Indeed, we found that YAP was required for astrocytic differentiation in mouse NSCs (Fig. 3), whereas in astrocytes it was necessary for cell proliferation (Figs 4, S3 and S5).

YAP appeared to be required for neocortical, but not hippocampal, astrogliogenesis (Fig. 5), although YAP was expressed in astrocytes in both brain regions. The mechanism underlying such a regional effect of YAP is unclear. One recent study has shown that gain of function of YAP by aberrant YAP activation leads to overexpansion of dorsal root ganglion glial populations (Serinagaoglu et al., 2015). In cultured human NSCs, YAP mediates astrocyte differentiation as a downstream signaling protein of the stretch-activated ion channel PIEZO1 (Pathak et al., 2014). Our results are consistent with these previous studies. We are also aware of reports that YAP regulates neural progenitor cell numbers in the developing neural tube of chick and *Xenopus* embryos and the mouse hippocampus, as shown in YAP gain- or loss-of-function assays (Cao et al., 2008; Gee et al., 2011; Lavado et al., 2013; Piccolo et al., 2014). However, our results showed normal neocortical neurogenesis in culture and in P0-P1 *Yap*^{nestin}-CKO mice (Figs 3, 5, 6 and S6). Again, the differing observations

Development (2016) 143, 2398-2409 doi:10.1242/dev.130658

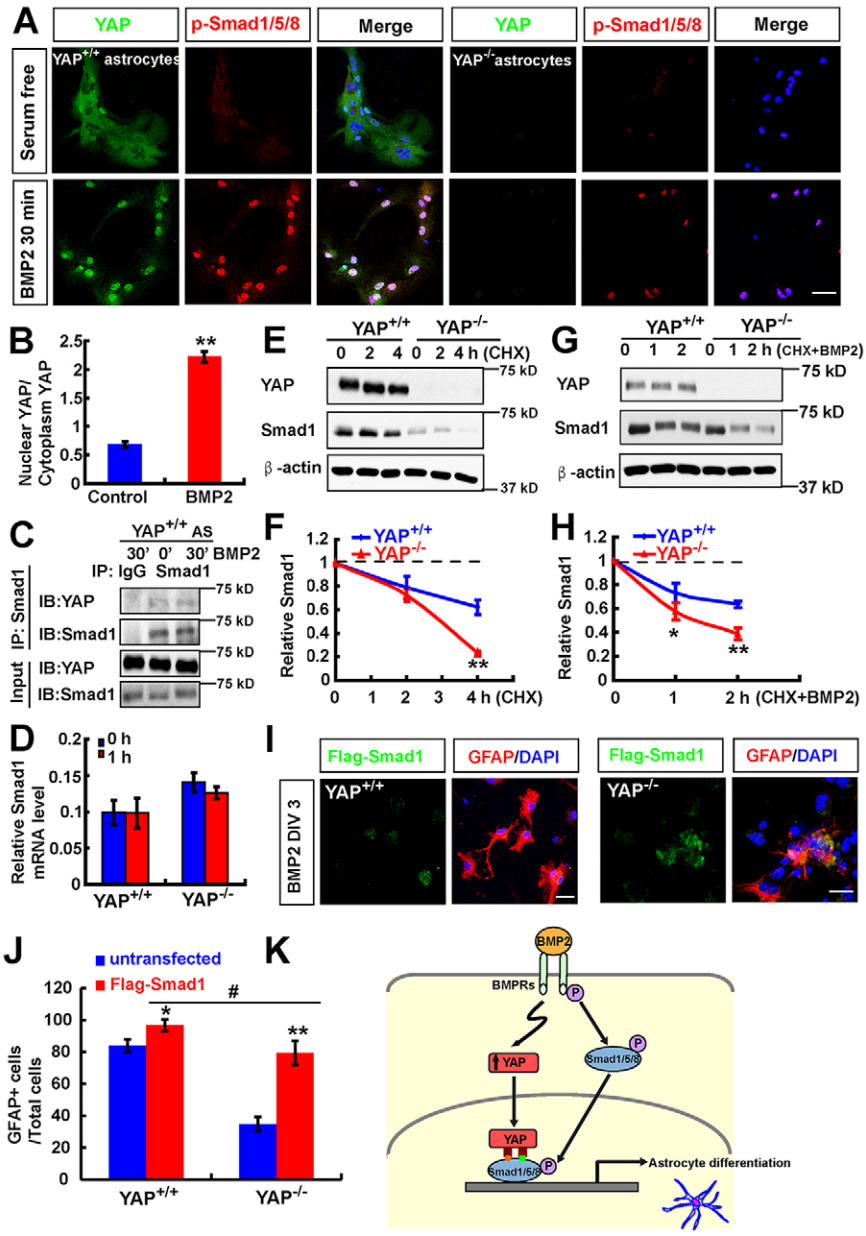

Fig. 8. YAP stabilizes the BMP2-SMAD1 signaling. (A) Double immunostaining analysis of YAP (green) and pSMAD1/5/8 (red) in WT and YAP-deficient astrocytes before and after BMP2 treatment (100 ng/ml). (B) Quantitative analysis of the ratio of nuclear to cytoplasmic YAP in astrocytes before and after BMP2 treatment. (C) Western blot showing results of nuclear protein complex co-IP assays in WT astrocytes before and after BMP2 treatment (100 ng/ml). (D) RT-PCR analysis of the *Smad1* mRNA level in astrocytes before and after BMP2 treatment (100 ng/ml). (E) Western blot showing YAP and SMAD1 levels in WT and YAP-deficient astrocytes before and after CHX (100 µM) treatment at the indicated time points. (F) Quantitative analysis of relative SMAD1 levels as shown in E (n=3 per group, normalized to 0 h). (G) Western blot showing YAP and SMAD1 levels in WT and YAP-deficient astrocytes before and after CHX (100 µM) plus BMP2 (100 ng/ml) treatment at the indicated time points. (H) Quantitative analysis of relative SMAD1 levels as shown in G (n=3 per group, normalized to 0 h). (I) Double immunostaining analysis of Flag (green) and GFAP (red) in WT and YAP-deficient NSCs transfected with Flag-SMAD1 3 days after BMP2 treatment (100 ng/ml). DIV, days *in vitro*. (J) Quantitative analysis of GFAP$^+$ cells in WT and YAP-deficient NSCs transfected with Flag-SMAD1 or untransfected under BMP2 treatment (n=6 each group). (K) Model of YAP functions in neocortical astrocytic differentiation. BMP2 treatment promotes YAP nuclear translocation, and the nuclear/active YAP interacts with and stabilizes SMAD1 and is required for BMP2-induced pSMAD1/5/8 signaling and astrocytic differentiation. Data are mean±s.e.m. *P<0.05, **P<0.01, compared with control group; $^{\#}P$<0.05, compared with WT control group after BMP2 treatment; Student's t-test. Scale bars: 20 µm.

might result from the different species (mouse versus chick) or brain regions (neocortex versus hippocampus) examined. Astrocytes play a key role in promoting neuronal survival (Sofroniew and Vinters, 2010). Although *Yap* deletion did not affect neurogenesis at birth, our results showed death of neocortical neurons at P7, which might be a consequence of decreased astrogliogenesis in the *Yap* mutant brain, as YAP was not expressed in neocortical neurons (Fig. 1C,G).

BMPs are members of the transforming growth factor beta (TGFβ) superfamily of signaling ligands (Bond et al., 2012) and play dynamic roles in neurogenesis and astrogliogenesis (Gross et al., 1996; Bond et al., 2012; Mallamaci, 2013). During late embryonic and early postnatal periods, BMP signaling promotes astroglial differentiation (Gross et al., 1996; Mehler et al., 2000; Mallamaci, 2013). Our results indicate that YAP in NSCs and astrocytes was activated by BMP2 and stabilized SMAD1 in the nucleus. This effect was required for neocortical astrogliogenesis. It is of interest to note that, in HEK293 or Eph4 cells, YAP is found to interact with SMADs in the nucleus to modulate BMP-SMAD1 or TGF-SMAD2 signaling (Alarcón et al., 2009; Aragon et al., 2011; Nallet-Staub et al., 2015; Narimatsu et al., 2015). In mouse embryonic stem cells, YAP promotes SMAD1-dependent transcription and is required for BMP2 suppression of neural differentiation (Alarcón et al., 2009). Our results are in line with these reports, revealing the importance of YAP regulation of BMP2-SMAD1 signaling in various cell types.

In summary, we provide evidence for YAP function in promoting neocortical astrocyte proliferation and differentiation during mouse development, which is likely to be due to YAP stabilizing BMP2-SMAD1 signaling.

MATERIALS AND METHODS

Mouse breeding and genotyping

Yap^{nestin}-CKO and *Yap*^{GFAP}-CKO mice were generated by crossing the floxed *Yap* allele (*Yap*$^{f/f}$) with nestin-Cre or GFAP-Cre transgenic mice (from The Jackson Laboratory; donated by Dr Rudiger Klein and Dr Albee Messing, respectively), maintained in a C57BL/6 strain background. *Yap*$^{f/f}$

Development (2016) 143, 2398-2409 doi:10.1242/dev.130658

mice were generated as previously described (Zhang et al., 2010; Wang et al., 2014). *Yap*^{nestin}-CKO mice survived the early postnatal stages, but after P8 they displayed marked growth retardation and died at ∼P25. The use of experimental animals has been approved by the IACUC at Georgia Regents University in accordance with NIH guidelines.

Primary culture of astrocytes, neurons and NSCs and transfection

Primary astrocyte cultures were prepared from the cerebral neocortex of P0-P3 neonatal mice (after genotyping) as described previously with slight modifications (Su et al., 2009). Briefly, cerebral neocortex was removed, demembranated, chopped, and then incubated with 0.125% trypsin at 37°C for 20 min, and dissociated into a single-cell suspension by mechanical disruption. The cells were seeded on poly-L-lysine (0.1 mg/ml, Sigma-Aldrich)-coated culture flasks and incubated in DMEM containing 10% fetal bovine serum (FBS, Gibco). After 6-10 days, the cultures became confluent. Microglia and oligodendrocytes were removed by shaking at 250 rpm for 4-6 h. Astrocytes were subsequently detached and plated into poly-L-lysine-coated dishes or coverslips. The purity of GFAP^{+} cells in our culture system is greater than 94%.

For NSC culture, pregnant mice (E14.5) were sacrificed following an established protocol (Wang and Yu, 2013). Mouse neocortex was dissociated to achieve a single-cell suspension. The single-cell suspensions were grown in Neurobasal-A Medium (NB, Life Technologies) supplemented with B27 (Life Technologies), 2 mM L-glutamine (Life Technologies), bFGF (20 ng/ml, Gibco) and EGF (20 ng/ml, Gibco). In cases where monolayer NSCs were needed for immunostaining or other treatments, neurospheres at passage two or three were dissociated into single cells and seeded onto poly-L-ornithine- and fibronectin-coated plates (Sigma). For NSC differentiation experiments, neurospheres were plated on poly-L-ornithine-coated coverslips under DMEM+10% FBS for 24 h or NB+2% B27 for 48-72 h. For NSC transfection, we used the NSC Nucleofector Kit (Amaxa) according to the manufacturer's instructions. The Flag-SMAD1 plasmid was purchased from Addgene.

Western blot

Brain tissues or cultured cells were lysed in lysis buffer [50 mM Tris-HCl (pH 7.4), 150 mM NaCl, 1% NP-40, 0.5% Triton X-100, 1 mM phenylmethylsulfonyl fluoride (PMSF), 1 mM EDTA, 5 mM sodium fluoride, 2 mM sodium orthovanadate and protease inhibitor cocktail (Sigma, P8340)] for 30 min on ice and centrifuged at 12,000 rpm (15,100 ***g***) for 20 min, and protein concentration was determined using a BCA protein assay kit (Thermo). Proteins were separated by 8%-12% SDS-PAGE and transferred onto nitrocellulose membrane. Blotted membranes were blocked in 10% skimmed milk at room temperature for 1 h and incubated with primary antibody overnight at 4°C, rinsed and incubated for 1 h at room temperature with an appropriate horseradish peroxidase-conjugated secondary antibody [1:5000, Bio-Rad, #170-6515 (goat anti-rabbit), #170-6516 (goat anti-mouse)] or Alexa Fluor 680/790 fluorescent secondary antibody [(1:20,000, Invitrogen, A21109 (goat anti-rabbit), A11357 (goat anti-mouse)]. Primary antibodies included mouse monoclonal anti-YAP (1:1000, WH0010413M1, Sigma), anti-GFAP (1:1000, MAB360, Millipore), anti-Tuj1 (1:500, T8660, Sigma), anti-nestin (1:1000, MAB353, Millipore), rabbit polyclonal anti-BLBP (1:1000, Ab32423, Abcam), anti-pYAP Ser127 [1:1000, #4911, Cell Signaling Technology (CST)], anti-pSMAD1/5/8 (1:1000, #13820, CST) and anti-SMAD1 (1:1000, #9743, CST). β-actin as a loading control was detected alongside the experimental samples (1:7000, A2228, Sigma). For chemiluminescence, protein bands detected by ECL (Pierce) were scanned into images and analyzed using ImageJ software (NIH). For fluorescence (Fig. 7C and Fig. 8E,G), images were acquired using the Odyssey Imaging System (LI-COR) and analyzed by Image-Pro analysis software (Media Cybernetics).

Nuclear complex co-immunoprecipitation (co-IP)

For co-IP experiments of SMAD1 and YAP, primary cultured astrocytes were starved with DMEM without serum for at least overnight before BMP2 treatment. After BMP2 (100 ng/ml) treatment, nuclear extracts were harvested for co-IP assays with anti-SMAD1 antibody (1:100, CST, #9743) using the Nuclear Complex co-IP Kit (Active Motif) according to the provided protocol.

Immunostaining

For brain tissue section staining, brains of E14-E16 and P0-P1 mice were removed and fixed in fresh 4% paraformaldehyde (PFA) for 2 days, and older mouse brains were removed and fixed in 4% PFA for 2 days after transcardial perfusion. Then brains were dehydrated in 15%, then 30% sucrose in PBS for 1-2 days, and cryopreserved in O.C.T. compound (SAKURA, #4583) for brain sections. Sections (20-30 µm) were cut on a freezing microtome and immediately processed for immunostaining by 1 h blocking in 10% BSA plus 0.3% Triton X-100 at room temperature, overnight incubation with primary antibodies at 4°C, and 1 h incubation at room temperature with appropriate secondary antibodies [1:500, Molecular Probes, A21202, A10036 (donkey anti-mouse), A21207, A21206 (donkey anti-rabbit), A11055 (donkey anti-goat)].

For cultured cell staining, cells were fixed with fresh 4% PFA in 0.1 M PBS (pH 7.4) for 20 min. After washing with PBS, cells were permeabilized with 0.1% Triton X-100 in 0.1 M PBS for 5 min, followed by incubation in blocking buffer (5% BSA and 0.1% Triton X-100 in 0.1 M PBS, pH 7.4) for 1 h, and incubated overnight at 4°C with primary antibodies diluted in the blocking buffer. Cells were washed three times with PBS and incubated for 1 h at room temperature with an appropriate fluorescence-conjugated secondary antibody [1:500, Molecular Probes, A21202, A10036 (donkey anti-mouse), A21207, A21206 (donkey anti-rabbit)]. Primary antibodies were rabbit polyclonal antibodies against nestin (1:200, SAB4200394, Sigma), BLBP (1:300, Ab32423, Abcam), Ki67 (1:200, AB9260, Millipore), PH3 (1:200, 06-570, Millipore), GFAP (1:500, AB5804, Millipore), GLAST (SLC1A3 or EAAT1; 1:200, AB416, Abcam), pSMAD1/5/8 (1:200, #13820, CST), Flag (1:2000, #14793, CST), YAP (1:200, #8418/D24E4, CST), CUX1 (1:200, M222, Santa Cruz), cleaved caspase 3 (1:100, #9661, CST), TBR1 (1:200, AB10554, Millipore) or TBR2 (1:400, AB2283, Millipore), or with monoclonal antibodies against YAP (1:200, WH0010413M1, Sigma), GFAP (1:500, MAB360, Millipore), NeuN (1:500, MAB377, Millipore), MAP2 (1:500, AB5622, Millipore), Tuj1 (1:500, T8660, Sigma) and nestin (1:1000, MAB353, Sigma), or with goat polyclonal antibodies against aldolase C (1:500, SC-12065, Santa Cruz).

Sections or cells were stained with DAPI (1:1000, Molecular Probes) to visualize the nucleus. Fluoro-Jade C was purchased from Millipore, and staining followed the provided protocol. Images were acquired on a Zeiss confocal system (FM300) using a multi-track configuration and processed using Zeiss confocal software and Adobe Photoshop CS 8.0 software.

BrdU injection and staining

For BrdU incorporation experiments, BrdU (100 µg/kg in PBS, Sigma) was administered by intraperitoneal injection at E14.5 (sacrificed at P0), P1 or P7 (sacrificed after 2 h). Brain sections were treated with 1 M HCl on ice for 10 min, then 2 M HCl at 37°C for 30 min, followed by treatment with 0.1 M $Na_2Ba_4O_7$ (pH 8.5) for 30 min at room temperature. After washing with PBS, brain sections were blocked with 10% BSA plus 1% Triton X-100. Monoclonal anti-BrdU antibody (1:200, Developmental Studies Hybridoma Bank) was incubated at 4°C overnight. Sections were then incubated with fluorescently conjugated Alexa Fluor 488 monoclonal IgG secondary antibody (1:500, Molecular Probes, A21202) for 45 min at room temperature. Images were acquired on a Zeiss confocal system using a multi-track configuration and processed using Adobe Photoshop CS 8.0 software.

Quantitative real-time PCR (qRT-PCR) analysis

For qRT-PCR, total RNA was extracted from astrocytes with Trizol reagent (Invitrogen), 1 µg of RNA was converted to cDNA using the Revert Aidfirst Strand cDNA Synthesis Kit (Thermo) in a 20 µl reaction, and then 0.5 µl product was used in a 20 µl reaction mixture containing SYBR GreenER qPCR SuperMix Universal (Invitrogen) with *Smad1* primers: forward, 5′-ACCTGCTTACCTGCCTCCTG-3′; reverse, 5′-CATAAGCAACCGCCT-GAACA-3′. The amplification cycle consisted of an initial step at 95°C for 5 min, followed by 40 cycles of denaturation at 95°C for 15 s and annealing at 60°C for 1 min, and extension at 72°C for 30 s. Samples were amplified

Development (2016) 143, 2398-2409 doi:10.1242/dev.130658

independently at least three times. Relative gene expression was converted using the $2^{-\Delta\Delta Ct}$ method against the internal control hypoxanthine guanine phosphoribosyl transferase 1 (*Hprt*): forward, 5′-TGGCCCTCTGTGTG-CTCAA-3′; reverse, 5′-TGATCATTACAGTAGCTCTTCAGTCTGA-3′.

Statistical analysis

All data presented represent results from at least three independent experiments. Statistical analysis was performed using Student's *t*-test or using ANOVA with pairwise comparisons. Statistical significance was defined as $P<0.05$.

Acknowledgements

We thank members of the W.-C.X. and L.M. laboratories for helpful discussions and suggestions.

Competing interests

The authors declare no competing or financial interests.

Author contributions

L.M., W.-C.X., Z.H. and J.Z. designed experiments and interpreted results; Z.H., J.H., J.P., Y.W. and G.H. performed experiments and analyzed data; W.-C.X and Z.H. wrote the manuscript.

Funding

This study was supported in part by grants from the National Institutes of Health [AG045781 to W.-C.X., L.M. and J.Z.] and U.S. Department of Veterans Affairs [BX000838 to W.-C.X. and L.M.]; and National Natural Science Foundation of China [81371350, 81571190]. Deposited in PMC for release after 12 months.

Supplementary information

Supplementary information available online at
http://dev.biologists.org/lookup/doi/10.1242/dev.130658.supplemental

References

Alarcón, C., Zaromytidou, A.-I., Xi, Q., Gao, S., Yu, J., Fujisawa, S., Barlas, A., Miller, A. N., Manova-Todorova, K., Macias, M. J. et al. (2009). Nuclear CDKs drive Smad transcriptional activation and turnover in BMP and TGF-beta pathways. *Cell* **139**, 757-769.

Aragon, E., Goerner, N., Zaromytidou, A.-I., Xi, Q., Escobedo, A., Massague, J. and Macias, M. J. (2011). A Smad action turnover switch operated by WW domain readers of a phosphoserine code. *Genes Dev.* **25**, 1275-1288.

Azzolin, L., Panciera, T., Soligo, S., Enzo, E., Bicciato, S., Dupont, S., Bresolin, S., Frasson, C., Basso, G., Guzzardo, V. et al. (2014). YAP/TAZ incorporation in the beta-catenin destruction complex orchestrates the Wnt response. *Cell* **158**, 157-170.

Bond, A. M., Bhalala, O. G. and Kessler, J. A. (2012). The dynamic role of bone morphogenetic proteins in neural stem cell fate and maturation. *Dev. Neurobiol.* **72**, 1068-1084.

Bonni, A., Sun, Y., Nadal-Vicens, M., Bhatt, A., Frank, D. A., Rozovsky, I., Stahl, N., Yancopoulos, G. D. and Greenberg, M. E. (1997). Regulation of gliogenesis in the central nervous system by the JAK-STAT signaling pathway. *Science* **278**, 477-483.

Cao, X., Pfaff, S. L. and Gage, F. H. (2008). YAP regulates neural progenitor cell number via the TEA domain transcription factor. *Genes Dev.* **22**, 3320-3334.

Chen, Q., Zhang, N., Gray, R. S., Li, H., Ewald, A. J., Zahnow, C. A. and Pan, D. (2014). A temporal requirement for Hippo signaling in mammary gland differentiation, growth, and tumorigenesis. *Genes Dev.* **28**, 432-437.

Fan, R., Kim, N.-G. and Gumbiner, B. M. (2013). Regulation of Hippo pathway by mitogenic growth factors via phosphoinositide 3-kinase and phosphoinositide-dependent kinase-1. *Proc. Natl. Acad. Sci. USA* **110**, 2569-2574.

Gavériaux-Ruff, C. and Kieffer, B. L. (2007). Conditional gene targeting in the mouse nervous system: Insights into brain function and diseases. *Pharmacol. Ther.* **113**, 619-634.

Ge, W.-P., Miyawaki, A., Gage, F. H., Jan, Y. N. and Jan, L. Y. (2012). Local generation of glia is a major astrocyte source in postnatal cortex. *Nature* **484**, 376-380.

Gee, S. T., Milgram, S. L., Kramer, K. L., Conlon, F. L. and Moody, S. A. (2011). Yes-associated protein 65 (YAP) expands neural progenitors and regulates Pax3 expression in the neural plate border zone. *PLoS ONE* **6**, e20309.

Gross, R. E., Mehler, M. F., Mabie, P. C., Zang, Z., Santschi, L. and Kessler, J. A. (1996). Bone morphogenetic proteins promote astroglial lineage commitment by mammalian subventricular zone progenitor cells. *Neuron* **17**, 595-606.

Gumbiner, B. M. and Kim, N.-G. (2014). The Hippo-YAP signaling pathway and contact inhibition of growth. *J. Cell Sci.* **127**, 709-717.

Guo, F., Ma, J., McCauley, E., Bannerman, P. and Pleasure, D. (2009). Early postnatal proteolipid promoter-expressing progenitors produce multilineage cells in vivo. *J. Neurosci.* **29**, 7256-7270.

He, F., Ge, W., Martinowich, K., Becker-Catania, S., Coskun, V., Zhu, W., Wu, H., Castro, D., Guillemot, F., Fan, G. et al. (2005). A positive autoregulatory loop of Jak-STAT signaling controls the onset of astrogliogenesis. *Nat. Neurosci.* **8**, 616-625.

Kriegstein, A. and Alvarez-Buylla, A. (2009). The glial nature of embryonic and adult neural stem cells. *Annu. Rev. Neurosci.* **32**, 149-184.

Lavado, A., He, Y., Pare, J., Neale, G., Olson, E. N., Giovannini, M. and Cao, X. (2013). Tumor suppressor Nf2 limits expansion of the neural progenitor pool by inhibiting Yap/Taz transcriptional coactivators. *Development* **140**, 3323-3334.

Lian, I., Kim, J., Okazawa, H., Zhao, J., Zhao, B., Yu, J., Chinnaiyan, A., Israel, M. A., Goldstein, L. S. B., Abujarour, R. et al. (2010). The role of YAP transcription coactivator in regulating stem cell self-renewal and differentiation. *Genes Dev.* **24**, 1106-1118.

Liu, H., Jiang, D., Chi, F. and Zhao, B. (2012). The Hippo pathway regulates stem cell proliferation, self-renewal, and differentiation. *Protein Cell* **3**, 291-304.

Mallamaci, A. (2013). Developmental control of cortico-cerebral astrogenesis. *Int. J. Dev. Biol.* **57**, 689-706.

Mehler, M. F., Mabie, P. C., Zhu, G., Gokhan, S. and Kessler, J. A. (2000). Developmental changes in progenitor cell responsiveness to bone morphogenetic proteins differentially modulate progressive CNS lineage fate. *Dev. Neurosci.* **22**, 74-85.

Mo, J.-S., Park, H. W. and Guan, K.-L. (2014). The Hippo signaling pathway in stem cell biology and cancer. *EMBO Rep.* **15**, 642-656.

Molofsky, A. V., Krenick, R., Ullian, E. M., Tsai, H.-h., Deneen, B., Richardson, W. D., Barres, B. A. and Rowitch, D. H. (2012). Astrocytes and disease: a neurodevelopmental perspective. *Genes Dev.* **26**, 891-907.

Morrison, S. J., Perez, S. E., Qiao, Z., Verdi, J. M., Hicks, C., Weinmaster, G. and Anderson, D. J. (2000). Transient Notch activation initiates an irreversible switch from neurogenesis to gliogenesis by neural crest stem cells. *Cell* **101**, 499-510.

Nallet-Staub, F., Yin, X., Gilbert, C., Marsaud, V., Ben Mimoun, S., Javelaud, D., Leof, E. B. and Mauviel, A. (2015). Cell density sensing alters TGF-beta signaling in a cell-type-specific manner, independent from Hippo pathway activation. *Dev. Cell* **32**, 640-651.

Narimatsu, M., Samavarchi-Tehrani, P., Varelas, X. and Wrana, J. L. (2015). Distinct polarity cues direct Taz/Yap and TGFbeta receptor localization to differentially control TGFbeta-induced Smad signaling. *Dev. Cell* **32**, 652-656.

Obayashi, S., Tabunoki, H., Kim, S. U. and Satoh, J.-i. (2009). Gene expression profiling of human neural progenitor cells following the serum-induced astrocyte differentiation. *Cell. Mol. Neurobiol.* **29**, 423-438.

Ohgushi, M., Minaguchi, M. and Sasai, Y. (2015). Rho-signaling-directed YAP/TAZ activity underlies the long-term survival and expansion of human embryonic stem cells. *Cell Stem Cell* **17**, 448-461.

Pan, D. (2010). The hippo signaling pathway in development and cancer. *Dev. Cell* **19**, 491-505.

Pathak, M. M., Nourse, J. L., Tran, T., Hwe, J., Arulmoli, J., Le, D. T. T., Bernardis, E., Flanagan, L. A. and Tombola, F. (2014). Stretch-activated ion channel Piezo1 directs lineage choice in human neural stem cells. *Proc. Natl. Acad. Sci. USA* **111**, 16148-16153.

Piccolo, S., Dupont, S. and Cordenonsi, M. (2014). The biology of YAP/TAZ: Hippo signaling and beyond. *Physiol. Rev.* **94**, 1287-1312.

Pijuan-Galito, S., Tamm, C. and Anneren, C. (2014). Serum Inter-alpha-inhibitor activates the Yes tyrosine kinase and YAP/TEAD transcriptional complex in mouse embryonic stem cells. *J. Biol. Chem.* **289**, 33492-33502.

Ramos, A. and Camargo, F. D. (2012). The Hippo signaling pathway and stem cell biology. *Trends Cell Biol.* **22**, 339-346.

Schlegelmilch, K., Mohseni, M., Kirak, O., Pruszak, J., Rodriguez, J. R., Zhou, D., Kreger, B. T., Vasioukhin, V., Avruch, J., Brummelkamp, T. R. et al. (2011). Yap1 acts downstream of alpha-catenin to control epidermal proliferation. *Cell* **144**, 782-795.

Serinagaoglu, Y., Paré, J., Giovannini, M. and Cao, X. (2015). Nf2–Yap signaling controls the expansion of DRG progenitors and glia during DRG development. *Dev. Biol.* **398**, 97-109.

Sofroniew, M. V. and Vinters, H. V. (2010). Astrocytes: biology and pathology. *Acta Neuropathol.* **119**, 7-35.

Su, Z., Yuan, Y., Chen, J., Cao, L., Zhu, Y., Gao, L., Qiu, Y. and He, C. (2009). Reactive astrocytes in glial scar attract olfactory ensheathing cells migration by secreted TNF-alpha in spinal cord lesion of rat. *PLoS ONE* **4**, e8141.

Tamm, C., Bower, N. and Anneren, C. (2011). Regulation of mouse embryonic stem cell self-renewal by a Yes-YAP-TEAD2 signaling pathway downstream of LIF. *J. Cell Sci.* **124**, 1136-1144.

Temple, S. (2001). The development of neural stem cells. *Nature* **414**, 112-117.

Varelas, X. (2014). The Hippo pathway effectors TAZ and YAP in development, homeostasis and disease. *Development* **141**, 1614-1626.

Wang, J. and Yu, R. K. (2013). Interaction of ganglioside GD3 with an EGF receptor sustains the self-renewal ability of mouse neural stem cells in vitro. *Proc. Natl. Acad. Sci. USA* **110**, 19137-19142.

Development (2016) 143, 2398-2409 doi:10.1242/dev.130658

Wang, Y., Hu, G., Liu, F., Wang, X., Wu, M., Schwarz, J. J. and Zhou, J. (2014). Deletion of yes-associated protein (YAP) specifically in cardiac and vascular smooth muscle cells reveals a crucial role for YAP in mouse cardiovascular development. *Circ. Res.* **114**, 957-965.

Yao, M., Wang, Y., Zhang, P., Chen, H., Xu, Z., Jiao, J. and Yuan, Z. (2014). BMP2-SMAD signaling represses the proliferation of embryonic neural stem cells through YAP. *J. Neurosci.* **34**, 12039-12048.

Yu, F.-X. and Guan, K.-L. (2013). The Hippo pathway: regulators and regulations. *Genes Dev.* **27**, 355-371.

Zhang, N., Bai, H., David, K. K., Dong, J., Zheng, Y., Cai, J., Giovannini, M., Liu, P., Anders, R. A. and Pan, D. (2010). The Merlin/NF2 tumor suppressor functions through the YAP oncoprotein to regulate tissue homeostasis in mammals. *Dev. Cell* **19**, 27-38.

Zhang, W., Nandakumar, N., Shi, Y., Manzano, M., Smith, A., Graham, G., Gupta, S., Vietsch, E. E., Laughlin, S. Z., Wadhwa, M. et al. (2014). Downstream of mutant KRAS, the transcription regulator YAP is essential for neoplastic progression to pancreatic ductal adenocarcinoma. *Sci. Signal.* **7**, ra42.

Zhao, B., Wei, X., Li, W., Udan, R. S., Yang, Q., Kim, J., Xie, J., Ikenoue, T., Yu, J., Li, L. et al. (2007). Inactivation of YAP oncoprotein by the Hippo pathway is involved in cell contact inhibition and tissue growth control. *Genes Dev.* **21**, 2747-2761.